

El Niño and La Niña: Causes and Global Consequences

Michael J McPhaden

Volume 1, **The Earth system: physical and chemical dimensions of global environmental change**,
pp 353–370

Edited by

Dr Michael C MacCracken and Dr John S Perry

in

Encyclopedia of Global Environmental Change

(ISBN 0-471-97796-9)

Editor-in-Chief

Ted Munn

This is a US Government Work and is in the public domain in the United States of America

El Niño and La Niña: Causes and Global Consequences

Michael J McPhaden

National Oceanic and Atmospheric Administration,
Seattle, WA, USA

El Niño is a warming of the tropical Pacific that occurs roughly every three to seven years and lasts for 12–18 months. It is dynamically linked to the Southern Oscillation, a see-saw in surface atmospheric pressure between the Australian–East Asian region and the eastern tropical Pacific. During El Niño, the trade winds weaken along the equator as atmospheric pressure rises in the western Pacific and falls in the eastern Pacific. Weakened trade winds allow warm surface water, normally confined to the western Pacific, to migrate eastward. Wind-driven upwelling, a process that brings cold water to the surface along the equator and along the west coasts of North and South America, is also greatly reduced, causing sea surface temperatures to rise. Upwelled waters are rich in nutrients that support biological productivity, so that reduced upwelling adversely affects marine ecosystems and economically valuable fish stocks.

In the atmosphere, deep cumulus clouds and heavy rains typically occur in the western Pacific over the warmest surface waters. As these waters migrate eastward during El Niño, so does the heavy rainfall. Condensation of water vapor into liquid water releases heat into the middle and upper troposphere. This heat provides a source of energy to drive global wind fields that extend El Niño's influence to remote parts of the planet. Altered circulation patterns produce droughts, floods, unusual storminess, heat waves, and other weather extremes that have serious social, economic, and public health consequences. However, El Niño can also have a positive influence on weather, such as bringing milder winters to North America and suppressing Atlantic hurricane formation.

La Niña is a climatological phenomenon akin to El Niño, but with opposite tendencies in the tropical Pacific Ocean and atmosphere. La Niña is characterized by stronger than normal trade winds and colder than normal tropical Pacific sea surface temperatures. It is also characterized by unusually high surface atmospheric pressure in the eastern tropical Pacific and low surface pressure in the western tropical Pacific in association with the Southern Oscillation. La Niña's effects on global weather are roughly opposite to those of El Niño. As a result, El Niño, La Niña and Southern Oscillation are often referred to collectively as El Niño/Southern Oscillation (ENSO), a cycle that oscillates year-to-year between warm, cold and neutral states in the tropical Pacific.

*After the disastrous 1982–1983 El Niño, which was neither predicted nor even detected until nearly at its peak, a 10-year international scientific research program was undertaken between 1985–1994 to improve the understanding, detection, and prediction of ENSO-related variability (see **TOGA (Tropical Ocean Global Atmosphere)**, Volume 1). New networks of moored and drifting buoys, island and coastal tide gauges, and ship-based measurements were initiated. Satellites provided global observations of the ocean and the atmosphere. Computer models were developed to forecast El Niño and La Niña events with lead times of up to one year. Scientific progress in these areas was highlighted during the 1997–1998 El Niño, which by some measures was the strongest on record. This El Niño was monitored day-by-day at a level of detail never before possible. In addition, early warning impending impacts, made possible by new data and forecasting techniques led to planning efforts in some parts of the world that helped to reduce the toll the El Niño, might otherwise have taken.*

The strength of the 1997–1998 El Niño, the tendency for more frequent El Niño events and less frequent La Niña events in the past 25 years, and the prolonged 1991–1995 El Niño have raised questions about the possible influence of global warming on the ENSO cycle. Some recent computer model simulations suggest that the ENSO cycle may be more energetic in a warmer world. However, no firm conclusions can be drawn at present because models used to simulate the interaction between global warming and ENSO are limited in their ability to accurately represent key physical processes. Also, available data are insufficient to unambiguously establish that recent changes in the ENSO cycle are outside the range of natural variability.

HISTORICAL BACKGROUND

El Niño in Spanish means *the child*, with specific reference to the Christ child. It was the name given by fishermen to a warm southward flowing coastal ocean current that occurred every year around Christmas time off the west coast of Peru and Ecuador. The term was later restricted to unusually strong warmings every few years that disrupted local fisheries, led to massive bird die offs, and brought torrential rains to the region. These coastal warmings and episodes of heavy rainfall have been linked by researchers over the past 40 years to much more extensive ocean warmings that occur across the width of the tropical Pacific basin (Figure 1). The term El Niño has now become synonymous with these extensive ocean warmings because of their impacts on global climate (Philander, 1990).

El Niño is coupled to an atmospheric phenomenon known as the Southern Oscillation, first defined by Sir Gilbert Walker in the early 20th century. Walker was an Englishman who was appointed director general of observatories

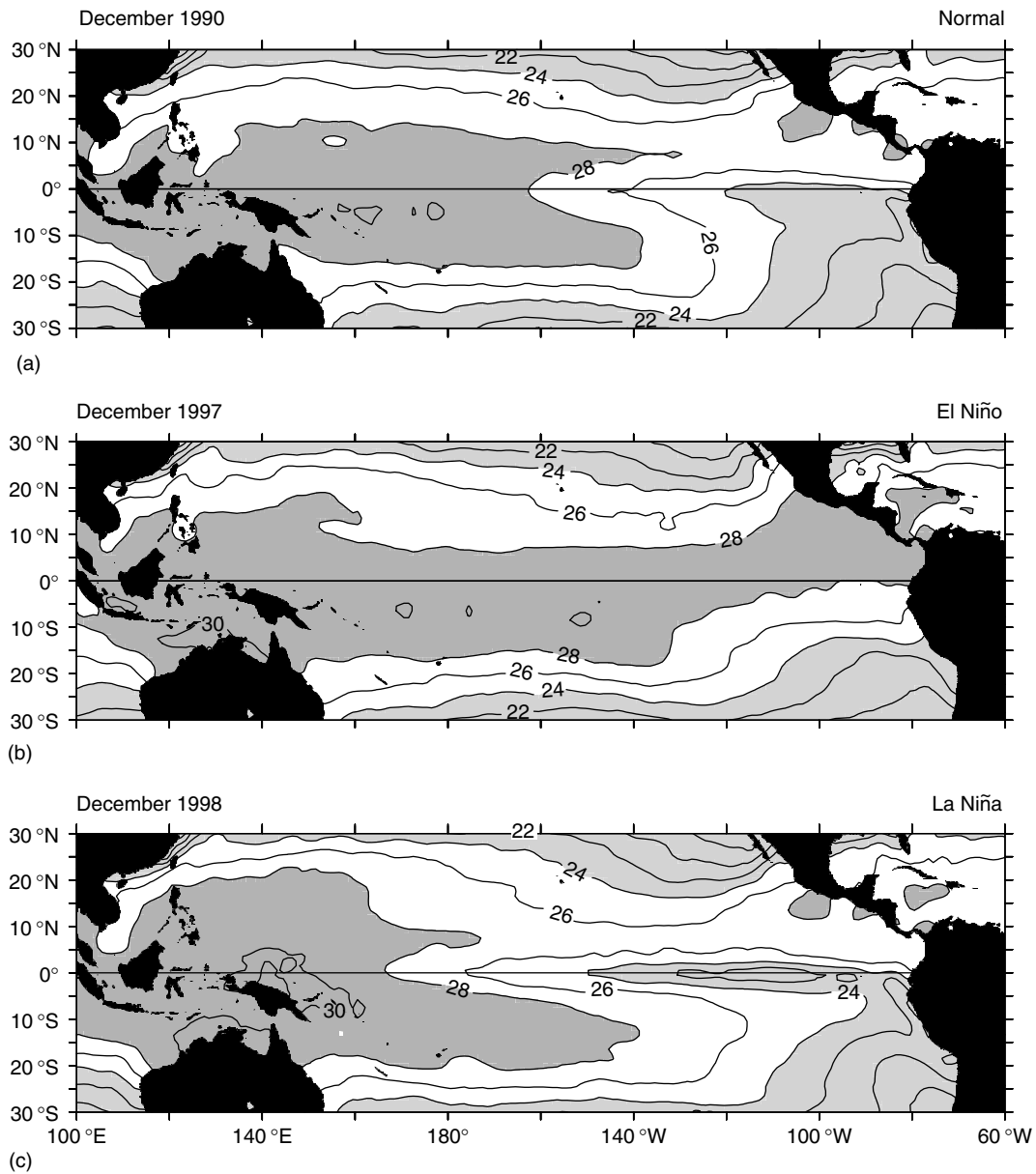


Figure 1 Monthly averaged sea surface temperature (in $^{\circ}\text{C}$) illustrating normal conditions in December 1990 (a), El Niño conditions in December 1997 (b), and La Niña conditions in December 1998 (c)

in India in 1904. He arrived in the wake of a devastating drought and famine that claimed more than a million lives in 1899–1900. Most of the rain in India falls during the summer monsoon. When the monsoons fail, the results can be disastrous for Indian agriculture. Walker believed that summer monsoon rainfalls might be predictable, so he set out to find possible precursors, gathering weather information from all over the world. In the 1920s and 1930s, he published a series of papers describing a year-to-year see-saw in surface atmospheric pressure between the Eastern and Western Hemispheres (Figure 2). He found that when pressure was unusually

low over the Indian Ocean region and the western tropical Pacific, it was high east of the international date line in the southeastern tropical Pacific. This situation corresponded to periods of good monsoon rains in India. When this pressure pattern was reversed, with low pressures east of the date line and high pressures west of the date line, rainfall was deficient not only in India, but also in neighboring countries such as Australia and Indonesia.

Unfortunately, for Walker, variations in the Southern Oscillation lagged rather than led those associated with Indian summer monsoon rainfall, so that his index was

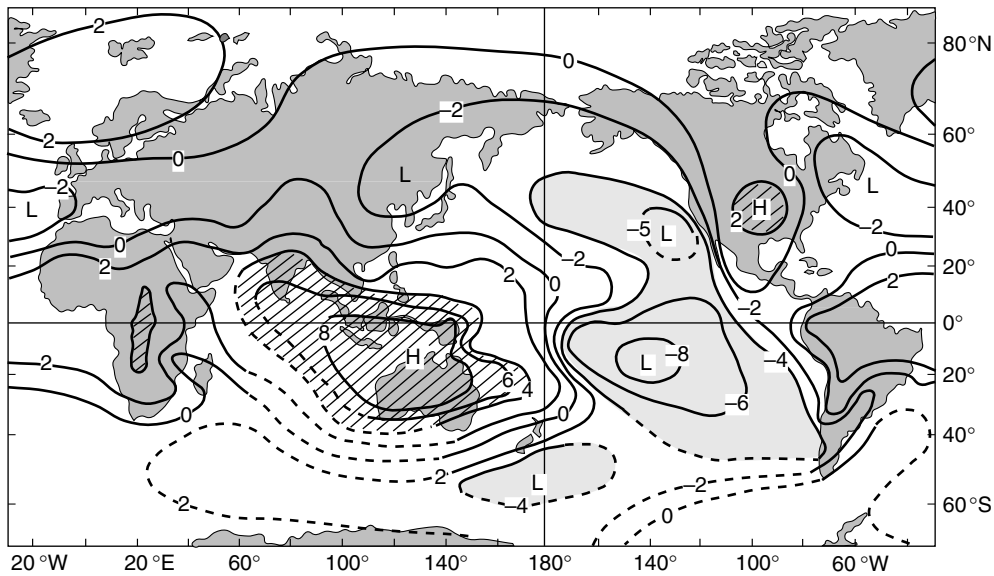


Figure 2 Spatial pattern of annual mean sea level pressure anomalies associated with the Southern Oscillation. Solid cross hatching indicates regions where sea level pressure varies in phase with Darwin, Northern Australia, and light shading indicates regions where sea level pressure varies out of phase with Darwin. Units are in correlation coefficient ($\times 10$), for which large absolute values indicate a more consistent relationship with Darwin (Trenberth and Shea, 1987)

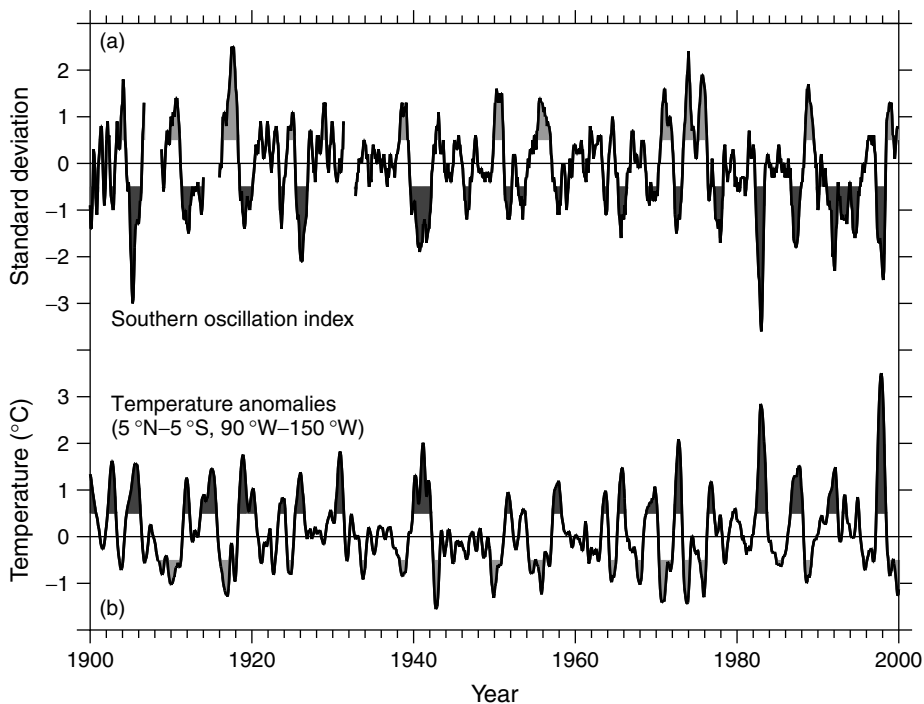


Figure 3 (a) SOI, which is a normalized difference between Tahiti, French Polynesia minus Darwin, Australia surface air pressure, after typical seasonal variations have been subtracted out. Periods of SOI greater in magnitude than 0.5 are shaded to emphasize the relationship with El Niño and La Niña episodes. Low SOI is associated with warm sea temperatures (El Niño), and high SOI with cold sea temperatures (La Niña). (b) Sea surface temperature anomalies (that is, deviations from normal) for the region 5°N – 5°S , 90°W – 150°W from 1900–1999. Positive anomalies greater than about 0.5°C indicate El Niño events. Negative anomalies less than about -0.5°C indicate La Niña events

not useful for monsoon predictions. Curiously, he also found that the low index phase of the Southern Oscillation was correlated with warm winters over Canada and dry conditions in parts of South Africa. His work was met with a great deal of skepticism though because he could not provide a physical explanation for the observed connections between the Southern Oscillation and climatic variations in widely separated parts of the globe. This skepticism was evident in his obituary, published in the *Quarterly Journal of the Royal Meteorological Society* (1959, p. 185):

Walker's hope was presumably not only to unearth relations useful for forecasting but to discover sufficient and sufficiently important relations to provide a productive starting point for a theory of world weather. It hardly seems to be working out like that.

Ironically, Walker died in 1958 during the 1957–1958 International Geophysical Year (IGY), the first truly international scientific study of the global oceans, atmosphere, and solid earth (see **IGY (International Geophysical Year)**, Volume 1). Intensive measurements were being undertaken in a coordinated effort to better understand the processes involved in shaping the global environment. As fate would have it, 1957–1958 coincided with a strong El Niño event. Measurements from the various observing systems deployed during the IGY stimulated Jacob Bjerknes to

examine how interactions between the ocean and the atmosphere in the tropical Pacific could affect weather patterns (see **Bjerknes, Jacob**, Volume 1). Bjerknes was a Norwegian meteorologist who emigrated to the US just before World War II. He had established his reputation in the early part of the century by making fundamental contributions to the understanding of fronts and weather systems at middle and high latitudes. Using IGY data in the 1960s, Bjerknes would be the first to identify the relationship between El Niño and the Southern Oscillation, to propose physical mechanisms by which they might interact, and to describe some of the effects of El Niño on North American weather.

The close connection between El Niño and the Southern Oscillation over the past 100 years can be seen in the strong inverse relationship between two commonly used indicators (Figure 3). The Southern Oscillation index (SOI) is based on departures from normal of surface atmospheric pressure at Tahiti, French Polynesia, and Darwin, Northern Australia. The difference of Tahiti minus Darwin pressure provides a measure of the pressure force that drives the trade winds across the Pacific basin. When this index is negative (low pressure at Tahiti relative to Darwin), the trade winds are weak. When the index is positive, the trade winds are strong.

A commonly used index for El Niño is the areal averaged sea surface anomaly (i.e., deviation from normal) in the

Box 1 El Niño and La Niña, Past and Present

El Niño and La Niña events generally last 12–18 months, and tend to be most fully developed during the Northern Hemisphere winter season. Thus, they often span two calendar years. Commonly used indices like those in Figure 3 show that El Niño events over the past 50 years occurred in 1951, 1953, 1957–1958, 1963, 1965–1966, 1969, 1972–1973, 1976–1977, 1982–1983, 1986–1987, 1991–1995 and 1997–1998. La Niña events of the past 50 years occurred in 1949–1950, 1955–1956, 1964, 1970–1971, 1973–1975, 1988–1989, 1995–1996 and 1998–2000. Weak cold events also occurred in 1967–1968 and 1984–1985, but these were not accompanied by positive values of the SOI.

Instrumental records available for identifying El Niño and La Niña years prior to the mid-19th century are very limited. However, it has still been possible to identify El Niño events in the distant past using anecdotal historical information from the reports of early explorers and settlers in those areas bordering the Pacific where in modern times El Niño consistently affects weather and climate. Quinn *et al.* (1987) produced a chronology of El Niño events going back to 1525 using historical reports of conditions from the coastal region and adjacent waters of northwestern South America. Their work suggests, e.g., that Francisco Pizarro's conquest of the Incas in 1531–1532 coincided with an El Niño event. Heavy rains and swollen rivers, which typically occur only during El Niño years in Peru, delayed Pizarro's advance through the countryside. On the other hand, the same

rains produced abundant vegetation, providing plentiful fodder for his horses, which were one of the chief tactical advantages (along with swords) that his small contingent of soldiers had over the natives.

Quinn (1992) extended this El Niño chronology back to 622 AD using maximum yearly Nile River flow data at Cairo, and related historical information on African droughts, floods, plagues and famines. Careful records of Nile stream flow were kept because it formed the basis of Egyptian agriculture for thousands of years. The stream flow records reveal year-to-year changes that can be related to variations in summer monsoon rains over the highlands of Ethiopia. These rains, and the stream flows they feed, are typically reduced in El Niño years.

It is possible to extend the record of ENSO time scale variations even further back in time by developing climate reconstructions using proxy data from tree rings, laminated lake sediments, glacier ice cores and tropical Pacific corals. These proxies preserve year-by-year records of environmental parameters related to physical climate, such as temperature, precipitation, or rainwater runoff. The relevant climate information is encoded in the chemical and isotopic composition of coral skeletons, the water content and chemistry of ice cores, the thickness and grain sizes of sediment layers, and the thickness and density of tree rings. Properly calibrated against modern instrumental records, proxy data allow investigations on ENSO-related climate variability to extend many thousands of years into the past.

region 5°N to 5°S , 90°W to 150°W . Large positive values of this index define warm El Niño conditions, while large negative values indicate cold La Niña conditions. It is evident that the warm surface temperatures are strongly linked to weak trade wind (negative values of the SOI) and vice versa. These indices show that the 1982–1983 El Niño and the 1997–1998 El Niño were the strongest of the 20th century.

El Niño events exhibit some common characteristics (such as unusually warm sea surface temperatures and weak trade winds in the tropical Pacific) that allow them to be classified as a distinct phenomenon (see Box 1). However, they often differ among themselves in duration, intensity and in the details of their development. No two El Niños are exactly alike, and the same is true of La Niña events. Thus, the ENSO cycle displays a degree of irregularity for which there is yet no simple explanation.

EL NIÑO PHYSICS AND THE ENSO CYCLE

To understand El Niño, we must first understand what is considered normal. Sunlight reaching the Earth's surface is more intense in the tropics than at higher latitudes, so that the warmest ocean temperatures are found near the equator. Air masses over warm tropical waters extract heat and moisture from the ocean, expand, become less dense than surrounding air, and ascend to higher altitudes. The rising air cools and condenses, producing towering cumulus clouds and heavy precipitation through a process referred to as deep convection. At upper levels of the troposphere (the lowest 10–12 km of the atmosphere affected by weather) these air masses flow poleward, then sink in regions of high surface pressure over the subtropical oceans of the Northern and Southern Hemispheres. The rising tropical air masses in turn are fed by air drawn in towards the equator near the surface from the subtropical high-pressure zones. This circulation cell on the meridional plane is called the Hadley circulation in honor of George Hadley, an 18th century British meteorologist who was the first to provide a theoretical explanation for it (*see Hadley Circulation*, Volume 1).

The equatorward flowing surface air masses are deflected westward because of the rotation of the Earth about its axis (the Coriolis effect). The result is easterly tradewind systems in the Northern and Southern Hemispheres. The northeast and southeast trade winds meet in the Intertropical Convergence Zone, situated on average about five to ten degrees of latitude north of the equator in the Pacific. This is a region of deep convection, cumulus cloud formation, and heavy rainfall that comprises the ascending branch of the Hadley circulation. A second zone of converging surface winds, the South Pacific Convergence Zone, is on average located several degrees south of the equator in the western tropical Pacific.

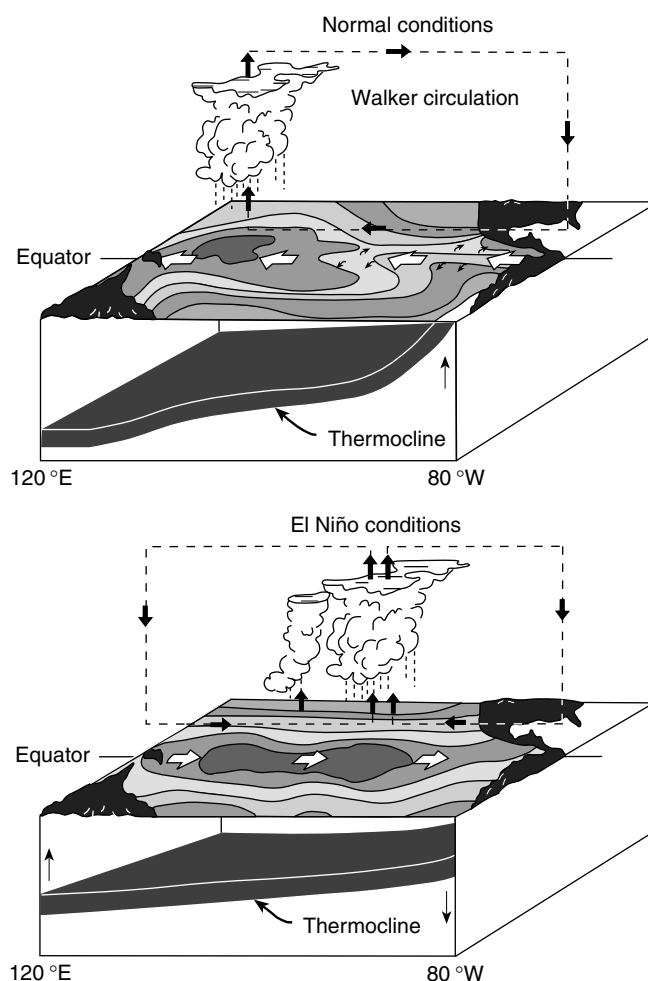


Figure 4 Schematic of normal and El Niño conditions in the equatorial Pacific

Along the equator, the trade winds normally drive surface flow westward in the south equatorial current (Figure 4). This current piles up the warm surface water in the western Pacific, and drains it from the eastern Pacific. The thermocline, which is the sharp vertical temperature gradient separating the warm surface layer from the cold deep ocean, is pushed down to a depth of 150 m in the west, but shoals to 50 m depth in the east. Sea level tends to mirror thermocline depth since water expands when heated. Thus, while the thermocline tilts downward towards the west along the equator, sea level rises to the west where it stands about 60 cm higher than in the eastern Pacific.

The relative shallowness of the thermocline in the eastern Pacific facilitates the upward transport of cold interior water by the trade winds, and a cold tongue develops in sea surface temperature from the coast of South America to near the international date line. The east–west surface temperature contrast reinforces the easterly trade winds, since low atmospheric surface pressure is associated with warm water in the west and high surface pressure with

Box 2 Equatorial Waves

One early theory for El Niño postulated that the winds blowing equatorward off the west coast of South America weakened during an El Niño event, so that coastal upwelling would be reduced and sea surface temperatures would rise. However, Klaus Wyrtki, an oceanographer at the University of Hawaii, demonstrated in the mid-1970s that winds along the coast of South America actually strengthened during El Niño (Wyrtki, 1975). He found instead that weakening of the tradewinds thousands of kilometers to the west in the central Pacific was related to the development of El Niño along the coast of South America some months later. Based on these results, Wyrtki suggested that large scale equatorial ocean waves were the mechanism by which wind variations in the central Pacific could lead to the onset of El Niño in the eastern Pacific.

Two classes of oceanic waves are important for understanding the cycle of El Niño and La Niña variations. One class is referred to as Kelvin waves, named after Lord Kelvin (William Thompson), a 19th century British physicist who was the first to theoretically predict such waves in rotating fluids. The other class is referred to as Rossby waves, named after Carl-Gustaf Rossby, a Swedish-born meteorologist who in

the 1930s first discovered this kind of wave in the atmosphere (see **Rossby Waves**, Volume 1; **Rossby, Carl-Gustaf**, Volume 1). Both types of wave are generated in the equatorial ocean by large-scale variations in surface winds.

Kelvin waves propagate eastward along the equator and Rossby waves propagate westward. They are evident below the surface as undulations of the thermocline, causing it to rise and fall by tens of meters as the waves pass by. Equatorial waves also affect sea level and the intensity and direction of ocean currents. The Earth's rotational forces trap these waves within several hundred kilometers of the equator in the open ocean, so they transfer energy very efficiently over many thousands of kilometers in the east–west direction.

Kelvin waves take about two months to cross the Pacific basin and Rossby waves take about six months to cross. When they reach the landmasses at the eastern and western boundaries of the ocean, they reflect back into the interior and, in the case of Kelvin waves, leak energy to higher latitudes along the west coasts of the Americas. The life cycle of these waves, evolving over many months and seasons in response to changing winds, are a critical aspect of ocean dynamics controlling the evolution of El Niño and La Niña events.

cooler water in the east. Also, as the trade winds flow from east to west, they pick up heat and moisture from the ocean. The warm, humid air mass becomes less dense and rises over the western Pacific warm pool where deep convection leads to towering cumulus clouds and heavy precipitation. Ascending air masses in this region of deep convection return eastward in the upper levels of the troposphere, then sink over the cooler water of the Eastern Pacific. Bjerknes labeled this atmospheric circulation pattern on the equatorial plane the Walker circulation in honor of Sir Gilbert Walker (see **Walker Circulation**, Volume 1).

Upwelling is a key oceanic process that regulates sea surface temperatures along the equator and along much of the west coast of the Americas. Wind-driven surface currents flow to the right of the winds in the Northern Hemisphere and to the left of the winds in the Southern Hemisphere because of the Coriolis force. Easterly trade wind-driven currents therefore flow poleward in opposite directions near the equator in the Northern and Southern Hemispheres. This divergent surface flow is fed from below by upwelled thermocline water to create the equatorial cold tongue (Figure 1). A similar process operates off the west coasts of the Americas. Equatorward winds on the eastern flanks of subtropical high-pressure systems drive surface waters offshore. These offshore flows are fed from below by cooler thermocline waters, which then lower coastal sea surface temperatures.

During El Niño, the trade winds weaken in the western and central equatorial Pacific as atmospheric pressure rises

in the west and falls in the east (Figure 4). Weakened trade winds generate waves in the ocean interior, which radiate along the equator both to the east and to the west away from the region of wind forcing (see Box 2). Over the course of a few months, these waves elevate the thermocline in the west and push it down in the east. In the cold tongue region, depression of the thermocline leads to surface warming as equatorial upwelling can no longer efficiently tap into the cold water reservoir below. Westward flow in the south equatorial current also weakens and reverses when the trade winds relax, allowing the western Pacific warm pool to migrate eastward. Sea level drops in the west and rises in the east in response to the redistribution of warm surface waters.

As sea surface temperatures warm east of the date line, the pattern of deep convection and precipitation also shifts eastward. This reinforces the reduction in trade wind intensity, because westerly winds flow into the convective center from the west. Pressure continues to fall in the east and rise in the west as the region of convection and rainfall migrates eastward. The system becomes locked in a positive feedback loop, with warming surface temperatures leading to weakened trade winds and vice versa. This positive feedback is eventually broken when the oceanic waves that elevated the thermocline in the western Pacific at the onset of the event bounce off the land masses bordering the western Pacific and reflect back toward the east. As the reflected waves propagate eastward along the equator, they elevate the thermocline and initiate surface cooling. Cooler surface waters in the eastern Pacific increase the east–west atmospheric pressure gradient

and the strength of the trade winds, which in turn reinforces surface cooling through intensified upwelling. These interactions between the ocean and the atmosphere terminate El Niño typically 12–18 months after its onset. The ocean returns to near normal conditions, or it may overshoot into a cold La Niña state.

While El Niño involves an intimate coupling of the atmosphere and the ocean, the two fluids respond to each other on very different time scales. The atmosphere is a thousand times less dense than the ocean, and therefore responds almost immediately to forcing from the ocean surface. The ocean is massive by comparison, so its dynamical response to atmospheric forcing is relatively sluggish. For example, thermocline depths may take many months to adjust to changing winds in the tropics, whereas atmospheric convection can develop within hours over warm surface water. It is the slow evolution of the upper ocean thermal field that provides the memory for the climate system in the tropical Pacific, and it is this thermal inertia that provides the basis for predictability of ENSO time scale variations.

EL NIÑO WEATHER IMPACTS

One impact of the eastward shift in rainfall along the equator during El Niño is that drought develops in Australia, Indonesia and neighboring countries. On the other hand, the island states of the central Pacific and the west coast of South America are inundated with heavy rains. Heavy rainfall bands normally situated north and south of the equator in the Intertropical Convergence Zone and the South Pacific Convergence Zone also shift equatorward as surface waters warm. These latitudinal shifts contribute to unusually heavy rains near the equator in the central and eastern Pacific, and to drought conditions at higher latitudes in regions such as New Caledonia and Fiji to the south, and Hawaii to the north.

Heat released into the troposphere from deep tropical convection is one of the principal driving forces for the global atmospheric circulation. Changes in the location of tropical heat sources during El Niño therefore lead to widespread changes in wind and weather patterns outside

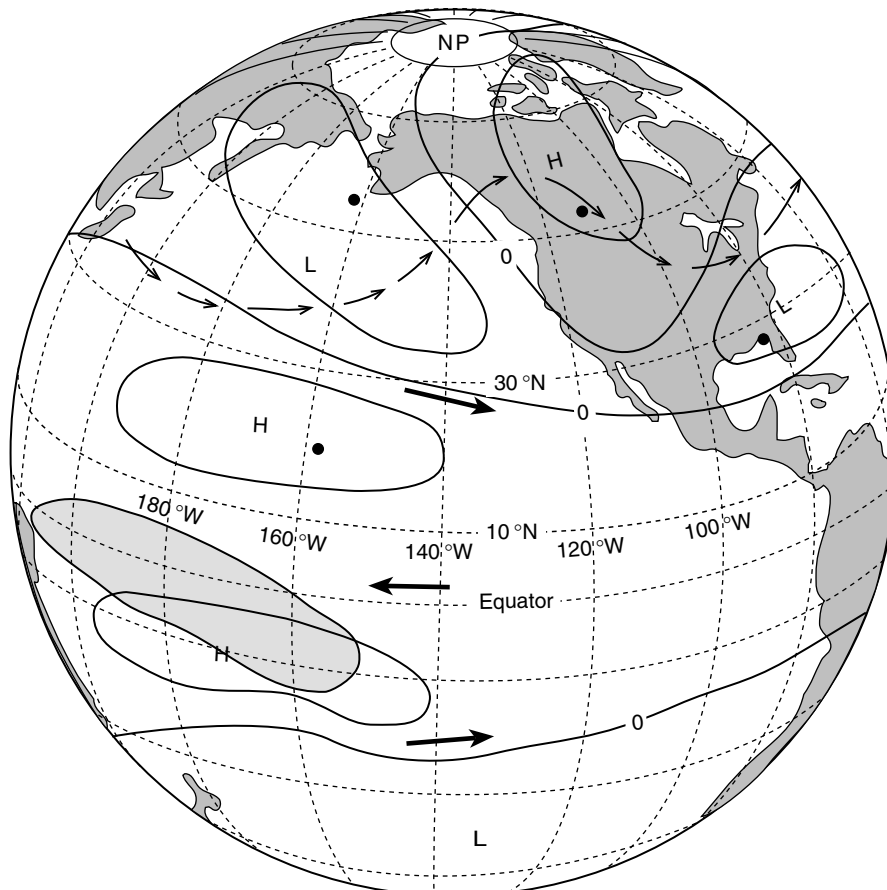


Figure 5 Schematic diagram of the PNA pattern of middle tropospheric pressure anomalies during Northern Hemisphere winter coinciding with an El Niño event. Dark arrows indicate strengthening of the subtropical westerly jet streams and, along the equator, weakening of the upper branch of the Walker circulation. Lighter arrows depict mid-tropospheric flows as distorted by the anomalous high and low pressure patterns. Rainfall and cloudiness are enhanced over the shaded region near the equator (Horel and Wallace, 1981)

the tropical Pacific. These remote effects of El Niño are referred to as teleconnections. In the extratropics, teleconnections are usually most pronounced during the winter season, though they are detectable in other seasons as well.

Anomalous tropospheric heating in the central tropical Pacific during El Niño generates quasi-stationary atmospheric wave trains that radiate poleward and eastward. In the Northern Hemisphere, these waves set up the Pacific North American Teleconnection Pattern, or (PNA) pattern, which is a series of high- and low-pressure centers extending from the central North Pacific to North America (Figure 5). During El Niño, the Aleutian low pressure center over the North Pacific deepens, high pressure develops over western North America, and low pressure prevails over the southeastern US. These pressure changes steer warmer air masses from southern latitudes into the

Pacific Northwest and southern Canada, so that much of Canada and the northwestern US tend to experience mild winters. Low pressure in the southeastern US associated with the PNA pattern brings wetter, cooler conditions to the states bordering the Gulf of Mexico. Similar wave trains are excited in the Southern Hemisphere, but they are weaker and more variable than those in the north.

Teleconnections also affect the subtropical jet streams which are swift air flows girdling the Earth at altitudes centered between about 10 000 m and 12 000 m (*see Teleconnection*, Volume 1). The eastward migration of deep convection during El Niño causes the core of these jet streams to intensify and shift southeastward in the central and eastern Pacific (Figure 5). The jet streams are a major influence on the location of storm tracks, so that southern California and northern Chile typically experience stormier

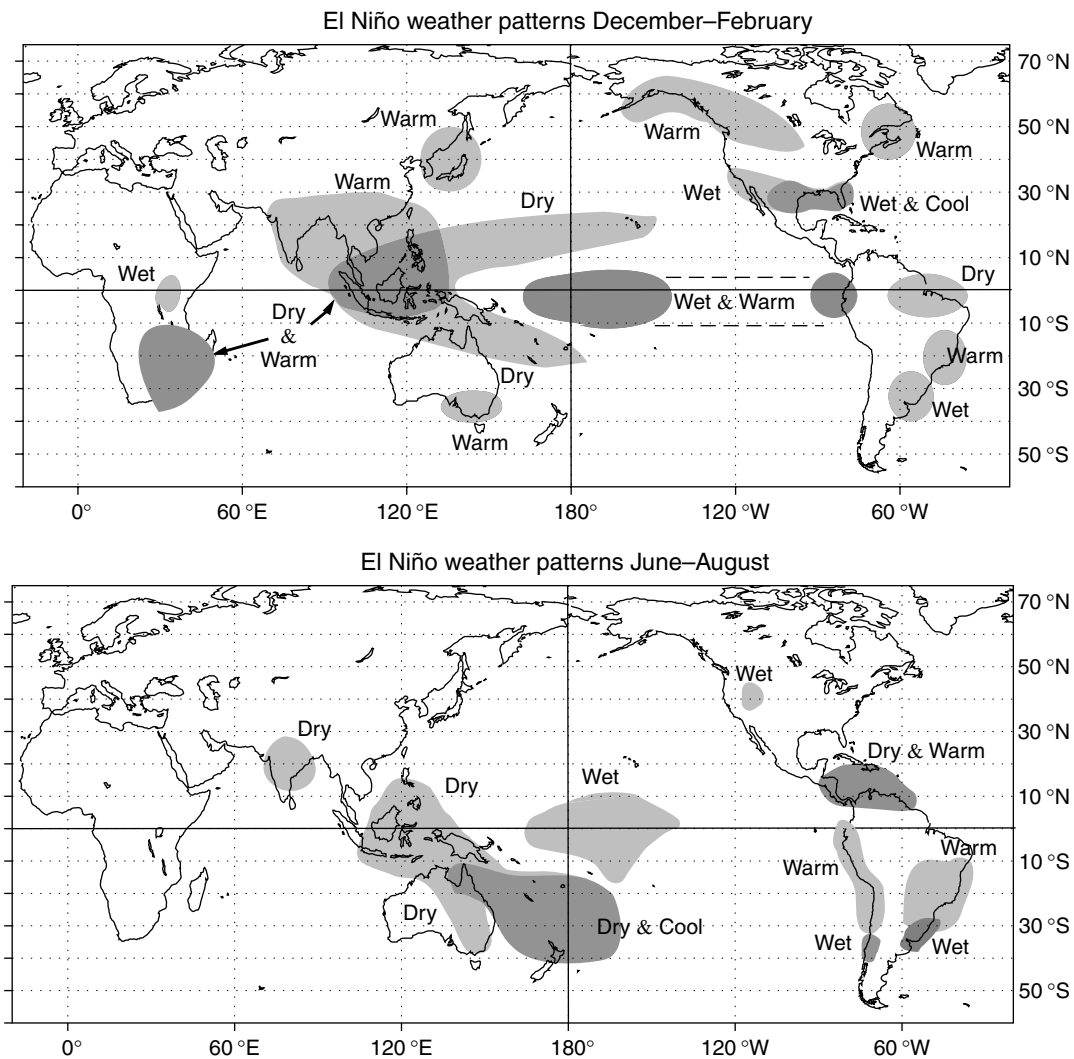


Figure 6 Schematic diagram showing temperature and precipitation anomalies associated with El Niño. To a first approximation, the impacts of La Niña are similar, but with opposite sign (Ropelewski and Halpert, 1987 and Halpert and Ropelewski, 1992)

and wetter weather in their respective winter seasons during El Niño.

Teleconnections affect surface conditions over land masses and the ocean. At extratropical latitudes of the North and South Pacific, for example, sea surface temperatures cool in response to intensified surface wintertime westerlies. Over land, changes in temperature and precipitation can affect soil moisture and evapotranspiration. These changes in surface conditions can feed back to the atmosphere, affecting the overall climatic response to El Niño forcing.

A global composite of typical rainfall and air temperature anomalies associated with El Niño is presented in Figure 6. In addition to effects already mentioned, El Niño years generally bring drought in northeastern Brazil, southern Africa, and the western Pacific, and wetter conditions to southern Brazil, Uruguay, Peru, and equatorial East Africa (Ropelewski and Halpert, 1987). Indian monsoon summer rains tend to be weaker during El Niño events, consistent with the strong relation between the Southern Oscillation and Indian monsoon rainfall noted by Walker.

El Niño also affects tropical storm frequency, intensity, and spatial distribution (Gray, 1984). In the Atlantic, 10 named tropical storms, of which six reach hurricane intensity (wind speeds greater than 33 ms^{-1}), form during a typical June to November hurricane season. However, during El Niño, an intensified subtropical jet stream shears off the top of fledgling storms before they fully develop. Thus, fewer tropical storms and hurricanes form, and those that do form tend to be weaker and shorter lived. The summer of 1997 was a particularly striking example of reduced Atlantic hurricane activity during El Niño. Only seven named storms formed, three of which reached hurricane intensity.

Intense tropical storms in other regions (referred to as hurricanes in the northeastern Pacific, typhoons in the northwestern Pacific, and cyclones in the Indian ocean and Southern Hemisphere) are affected more in terms of their spatial distribution and intensity than in terms of total numbers (*see Hurricanes, Typhoons and other Tropical Storms – Descriptive Overview*, Volume 1; *Hurricanes, Typhoons and other Tropical Storms – Dynamics and Intensity*, Volume 1). Heat from the underlying ocean surface is a major source of energy for intense tropical storms, which are almost always generated over waters warmer than 26°C . Therefore, extensive warming of the eastern Pacific during El Niño allows hurricanes to travel farther westward and northward and, in some cases, attain greater strength. Similarly, the eastward extension of warm tropical surface waters along the equator during El Niño expands the area over which typhoons and cyclones may spawn. Changes that can occur in tropical storm activity in the eastern Pacific during El Niño are exemplified by the 1997 season when hurricane Linda grew to record strength and hurricane Nora tracked far to the north, bringing heavy rains to normally arid northern Mexico and the southwestern US.

In the South Pacific during the 1982–1883 El Niño, ocean surface warming allowed six cyclones to strike French Polynesia, a region not usually prone to experiencing intense tropical storms (Canby, 1984).

El Niño affects the coastal zones of the Americas all the way to Alaska in the Northern Hemisphere and at least to central Chile in the Southern Hemisphere. When eastward propagating oceanic waves generated by weakening of the trade winds at the onset of El Niño reach the coast of South America, part of the wave energy is reflected back into the open ocean, but part also radiates northward and southward along the coasts. The coastal waves push the thermocline down and reduce the upwelling of cool water as they progress poleward. Within one to two months after the first equatorial waves reach South America, sea surface temperatures rise all along the coast to the north and south. North of central California, southerly surface winds related to the PNA pattern also contribute to coastal warming (Ramp *et al.*, 1997). These winds both bring warm subtropical air northward, and also drive on-shore ocean currents that converge at the coast to push the thermocline down.

The unusually thick layer of warm surface water along the west coast causes near shore sea levels to rise by 15–30 cm during El Niño. In addition, offshore winter storms associated with intensified jet streams in the subtropics can generate unusually high ocean swells and storm surges in coastal zones. Storm-generated surface waves and currents, and high tides, can add to already elevated sea levels high tides to cause severe coastal erosion. In communities with major shoreline development such as in southern California, the combined assault from high seas and heavy rains can lead to significant loss of property and life.

The impacts of El Niño on weather are most consistent from event to event in the tropical Pacific and bordering areas. Impacts are prominent, but less consistent, at higher latitudes and in other ocean basins where regional influences can become important. Thus, although El Niño increases the probability of a particular kind of weather pattern occurring in particular regions of the globe, actual impacts may vary from those expected for any given event (Trenberth *et al.*, 1998).

ECOSYSTEMS IMPACTS

Narrow coastal and equatorial upwelling zones account for much of the biological productivity in the world's oceans. One-celled plants known as phytoplankton are at the base of the aquatic food chain in these regions, and all higher organisms depend directly or indirectly on them as a food source. Upwelling ecosystems are rich in species diversity and abundance, including many types of phytoplankton, zooplankton, shellfish, crustaceans, fish, marine mammals,

and sea birds. Many of the fish and shellfish species such as tuna, anchoveta, sardines, squid, and shrimp are valuable commercially.

Primary productivity is the rate at which carbon is taken up by phytoplankton via photosynthesis. Nutrient limitation controls primary productivity in tropical and subtropical regions where sunlight is plentiful. The principal source for nutrients, away from river outflows and areas of significant coastal runoff, is the thermocline. Small organisms that have died near the surface decay and remineralize as they slowly sink out of the euphotic zone (the well lit upper layer of the ocean). Fecal pellets from larger organisms likewise sink and decompose at depth. These processes create a pool of nutrients and remineralized carbon in the thermocline which, when upwelled into the euphotic zone, are available for uptake by phytoplankton. Lateral flows in the thermocline may bring nutrients and carbon from great distances before they are upwelled, concentrating primary production in narrow equatorial and coastal zones.

During El Niño, ocean dynamical processes depress the thermocline in the eastern and central equatorial Pacific, and along the coasts of North and South America. The supply of nutrients to the euphotic zone drops or may be cut off entirely. Primary production decreases, with effects that ripple through the entire food chain (Barber and Chavez, 1984). Zooplankton that feed on phytoplankton decrease in abundance. Fish, sea birds and marine mammals die off or migrate to more productive regions in search of food. Undernourished sea birds and marine mammals may experience reproductive failures or abandon young when food becomes scarce. In extreme cases, decimated populations may require one or more years to fully rebound.

El Niño can also cause bleaching of tropical corals when water temperatures become too warm (Strong *et al.*, 2000) (*see Coral Reefs: an Ecosystem Subject to Multiple Environmental Threats*, Volume 2 and *Coral Bleaching (1997–1998)*, Volume 2). Corals thrive in a narrow range of temperatures between about 18 and 28 °C. At temperatures above the upper threshold, they expel symbiotic algae that reside in their polyps. The algae add color to healthy corals, and their metabolic by-products are essential for coral survival. Coral can recover from bleaching unless water temperatures remain too high for too long. The concern over lethal bleaching is that it threatens the vitality of coral reef ecosystems, which support local fisheries and provide tourist income. Massive and widespread coral bleaching occurred during 1998 in the Galapagos Islands, off the coast of Panama, in the Great Barrier Reef of Australia and elsewhere in the tropics in response to the exceptionally strong 1997–1998 El Niño. Decadal warming trends in tropical ocean temperatures contributed to this bleaching, by elevating background temperatures on which El Niño

warming was superimposed. These decadal trends, possibly related to global warming, have raised concerns about prolonged deterioration in the health of coral reefs.

El Niño can also dramatically affect fisheries, a particularly striking example of which was the collapse of the Peruvian anchoveta fishery following the 1972–1973 El Niño (Glantz, 2001). In the late 1960s and early 1970s, Peru was the most productive fishing nation in the world. The annual catch of anchoveta was over 10 million metric tons, one fifth of the global total. Most of the catch was exported for use as a feed supplement in poultry farms, with the exports accounting for nearly one third of Peru's foreign exchange earnings. Concerns were voiced at the time that overfishing might be depleting the stocks from sustainable levels. Those concerns proved to be well founded. Intense fishing pressure and extraordinarily high mortality rates during the 1972–1973 El Niño caused the fishery to crash. Effects were long lasting. For at least 10 years following the 1972–1973 El Niño, anchoveta landings ranged between only 1/10–1/3 the catch of 1970.

It was the collapse of the Peruvian anchoveta fishery that focused international attention on the socio-economic consequences of El Niño. A reduction in the supply of fishmeal caused many farmers in the US to switch from planting wheat to planting soybeans. Soy is an alternative source of poultry feed supplement and more lucrative than wheat as a cash crop. However, wheat harvests had declined in many nations, particularly the Soviet Union, because of widespread droughts in 1972. Staple food shortages developed in some regions and prices steeply increased for basic commodities in others. These events highlighted the role of climate in affecting global economies, and specifically focused attention on the need for a better understanding of the El Niño phenomenon.

DEVELOPMENT OF ENSO OBSERVING AND FORECASTING SYSTEMS

Research efforts in both oceanography and meteorology in the decade following the 1972–1973 El Niño gathered momentum, motivated by heightened awareness of El Niño's global socio-economic consequences, and the prospect that it might be predictable. It was recognized that advance warning of an impending El Niño would potentially be extremely valuable for either disaster preparedness or for exploiting opportunities created by altered environmental conditions. Thus, in the early 1980s, the international research community began mobilizing resources for a major 10-year study of El Niño. This study, called the Tropical Ocean-Global Atmosphere study, or (TOGA), took place from 1985–1994.

The 1982–1983 El Niño, the strongest in over 100 years, occurred as plans for TOGA were being formulated. This El Niño left a global swath of devastation in its wake. It had

not been predicted because El Niño forecasting capabilities had not yet been developed. Even more stunning to the research community, however, was that it was not even detected until nearly at its peak. At the time, most oceanographic data were available for analysis only months, or in some cases years, after they had been collected. A handful of scattered but more readily available ocean and weather data from islands and volunteer observing ships suggested the development of unusually warm conditions in mid-1982, but these reports were discounted as erroneous. One reason was that the 1982–1983 El Niño developed differently than expected from conventional wisdom. There had been no prior strengthening of the trade winds, and no warming off the west coast of South America in early 1982, both considered at the time to be necessary precursors of an impending El Niño. To complicate matters, eruptions of the Mexican volcano El Chichón in March–April 1982

injected a massive cloud of aerosols (dust, soot, and other fine particles) into the lower stratosphere, where prevailing winds spread it around the globe at low latitudes within weeks. This cloud of volcanic aerosols produced undetected cold biases of several degrees Celsius in satellite measurements of sea surface temperature. It was only after definitive reports were received from a research cruise in the eastern equatorial Pacific that the scientific community realized to what extent existing data sources and simplistic notions of El Niño evolution had misled them.

The lessons from this experience were clear: there was urgent need for improved monitoring, detection, and understanding of El Niño, as well as an urgent need to develop reliable El Niño forecast models. Observational requirements were met in part by utilizing data from a constellation of satellites viewing the Earth from space. However, satellites require Earth-based measurements for calibration

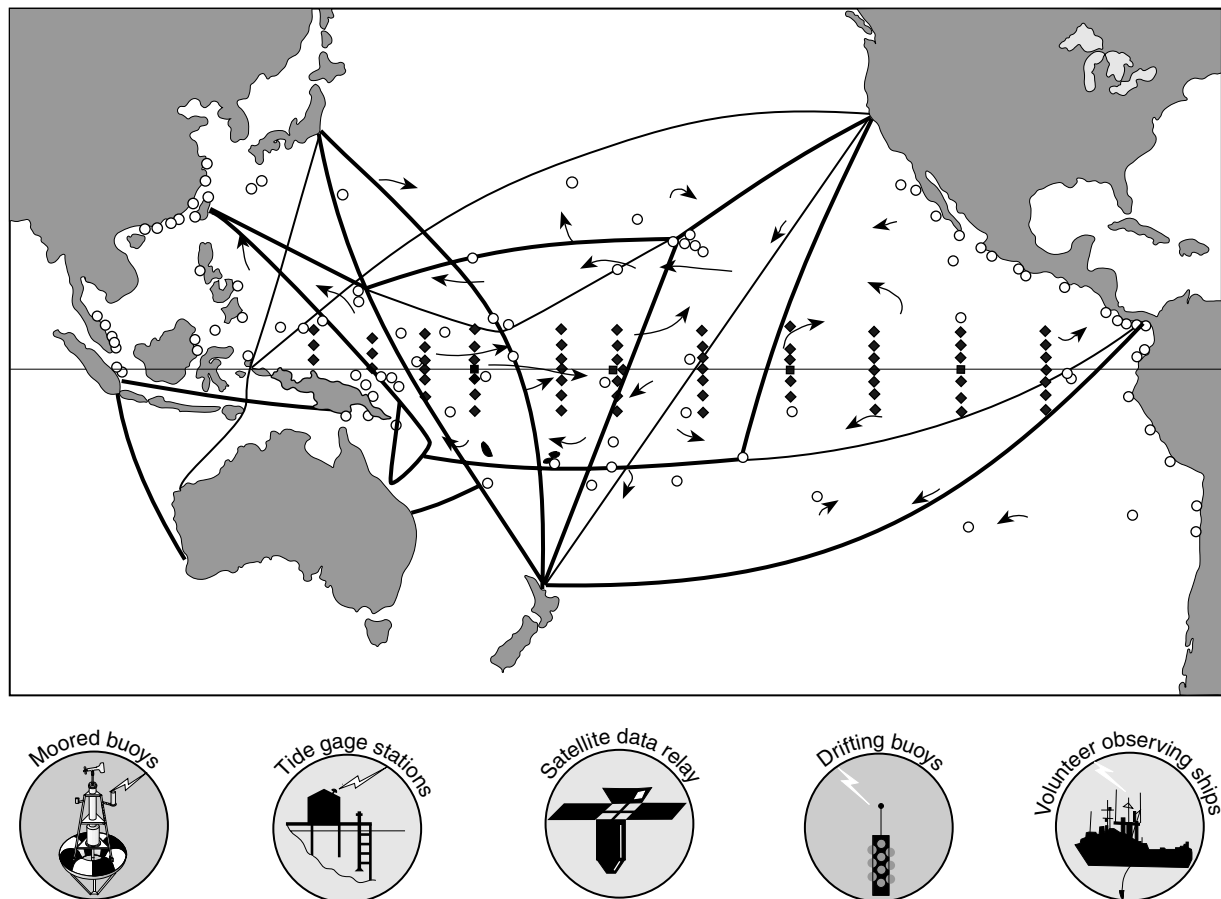


Figure 7 The ENSO Observing System. The four major elements of this observing system are; (1) a volunteer observing ship program for surface marine meteorological observations and ocean temperature profiles (shown by schematic ship tracks); (2) an island and coastal tide gauge network for sea level measurements (circles); (3) a drifting buoy network for sea surface temperatures and ocean currents (shown schematically by curved arrows); (4) a moored buoy array for wind, ocean temperature, and ocean current measurements (squares and diamonds). Thick ship track indicate repeat transects 11 or more times per year; thin ship track indicate repeat transects six to ten times per year. One schematic drifting buoy arrow represents 10 actual randomly distributed drifters (McPhaden *et al.*, 1998)

and verification. Also, satellites do not see below the ocean surface, where critical oceanic processes operate to produce El Niño events. An ocean observing system specifically designed for El Niño was therefore developed under the auspices of the TOGA program (McPhaden *et al.*, 1998) (see **TOGA (Tropical Ocean Global Atmosphere)**, Volume 1). It included an extensive network of moored buoys, drifting buoys, volunteer observing ships, and tide gauges (Figure 7). One of the most important attributes of this system was that most of the data were transmitted via satellite relay to shore stations within hours of collection. The observing system was implemented through an international collaborative effort spanning the full 10 years of TOGA, and was completed only in the last month of the program (December 1994). Continued after TOGA, it is now called the ENSO Observing System. The 1997–1998 El Niño was the first for which the ENSO Observing System was in place from start to finish, so that this event was not only among the strongest on record, but also the best ever documented (McPhaden, 1999).

Progress in the development of the ENSO Observing System has been paralleled in the development of ENSO forecast models (National Research Council, 1996). These models range from statistical approaches based on the average behavior of previous ENSO variations, to complex dynamical models that explicitly represent the physical processes at work in the coupled ocean-atmosphere system. The 1986–1987 El Niño was the first to be successfully predicted with these techniques, which have since undergone continual refinement and improvement. As one measure of success, many ENSO forecast models predicted that 1997 would be unusually warm in the tropical Pacific at least one to three seasons in advance (Barnston *et al.*, 1999). Long-range weather forecasting schemes that included information about tropical Pacific conditions during the 1997–1998 El Niño likewise had success in predicting surface air temperature and precipitation patterns in widely disparate parts of the globe months in advance. For instance, the forecast for wintertime precipitation and temperature issued by the National Centers for Environmental Prediction in Washington, DC, in the fall of 1997 were among the most accurate ever for the continental US.

Successful seasonal forecasts, unprecedented high definition ocean measurements from the ENSO Observing System, and record warmth in the tropical Pacific all combined to capture the attention of the public in 1997–1998. Media coverage was so intense that El Niño became a household word all over the world. As a result of the heightened public awareness about El Niño and its consequences, many individuals, municipalities, businesses, and in some cases national governments mobilized resources in an effort to prepare for El Niño's onslaught. It is likely that without the advance warning made possible by new measurement

and forecasting capabilities, the toll in terms of lives, property damage, and economic losses due to the 1997–1998 El Niño would have been much higher.

SOCIO-ECONOMIC IMPACTS OF THE 1997–1998 EL NIÑO

The 1997–1998 El Niño affected the lives of tens of millions of people around the globe. Significant disruptions were experienced in agriculture, forestry, fisheries, transportation, communications, power generation, public health and other climate-sensitive areas of human endeavor. Weather-related disasters and disease outbreaks during this El Niño claimed over 22 000 lives worldwide and caused US\$36 billion dollars in economic losses (Sponberg, 1999).

The 1997–1998 El Niño brought torrential rainfalls and flooding to parts of California, the southeastern US, equatorial East Africa and Chile. It was also responsible for severe droughts in Papua New Guinea, Indonesia, Central America, and northeastern Brazil (Supplee, 1999; WMO, 1999). Many regions experienced extensive crop failures and livestock losses due to these droughts and floods. Life-threatening food and drinking water shortages developed in New Guinea, prompting international relief efforts. In some drought-stricken regions, forest fires raged for months, devastating the countryside. The drought and fires in Indonesia produced deadly smog that covered an area one half the size of the continental US, causing widespread respiratory ailments, and contributing to airline and shipping disasters. Unusually low water levels in the lakes that feed the Panama Canal forced officials to restrict traffic through the waterway for the first time in 15 years.

Flood-contaminated water supplies in some regions contributed to outbreaks of cholera and dysentery. Stagnant pools of floodwater also provided ideal breeding grounds for mosquitos and other insects that spread infectious diseases like malaria and dengue fever. Public health emergencies developed in Southeast Asia, South America, and Africa as these diseases afflicted thousands of people.

Heavy rains and flooding from El Niño damaged or destroyed roads, bridges, buildings and phone and power lines in many parts of the globe. Thousands of individuals and families lost homes and personal property due to storms, floods, mud slides and land slides. Hydroelectric energy generation was curtailed in regions of severely reduced rainfall and stream flow. Many businesses lost income as a result of weather-related closures, commodity shortages or shifts in market demand for consumer goods. Tourism was affected because of extreme weather in areas such as southern California and Florida. The catch of Peruvian anchoveta fell sharply as in previous El Niño years, and the fishery was briefly closed by government decree

as a precautionary measure to limit further depletion of the remaining stock. Economic hardship followed severe declines in catch experienced in three of the four major fisheries (tuna, squid, sardine) off the west coast of Baja California.

Despite losses of life, property, and income, 1997–1998 El Niño produced some benefits as well (Changnon, 1999). Losses from Atlantic hurricanes were greatly reduced, as only one of three hurricanes that formed made landfall. Parts of the US Midwest and the Great Lakes region experienced the mildest winter in over 100 years, as temperatures warmed to record highs between November 1997 and February 1998. The milder than normal winter reduced heating bills, weather-related travel delays for the transportation industry, and deaths from exposure. It has been estimated that for the US as a whole, the 1997–1998 El Niño produced a net economic gain of about \$16 billion dollars and resulted in 650 fewer deaths than would have otherwise occurred.

Similarly, not all fisheries were hit hard by the 1997–1998 El Niño. Though severe declines in most commercial fisheries were experienced off the west coast of Baja California, these declines were partially offset by an eight-fold increase in the catch of more lucrative shrimp. Likewise, shrimp catch increased off the coast of Ecuador, with export revenues rising by 40% in 1997 (WMO, 1999). Northward migration of warm water fish species such as marlin, tuna and mahi-mahi was also a boom to the sport-fishing industry off the west coast of the US.

The 1997–1998 El Niño highlighted societal sensitivities and vulnerabilities to year-to-year climate fluctuations on a global scale. It also demonstrated that losses and gains are inherently unevenly distributed across economic sectors and national boundaries. Spurred in part by the dramatic consequences of this El Niño, new areas of interdisciplinary research are emerging to examine the use of El Niño-related climate information in economic planning and policy decisions. These efforts involve both social and physical scientists, with a focus on not only how forecasts are generated, but also how they are disseminated, interpreted, and acted upon.

LA NIÑA

La Niña is the cold phase of the ENSO cycle (Philander, 1990). It is characterized by stronger than normal trade winds, colder tropical Pacific sea surface temperatures, and positive values of the SOI (Figure 3). It represents a situation in which oceanic and atmospheric processes which give rise to normal conditions illustrated in Figure 4 are exaggerated, with deep convection and heavy rainfall along the equator shifted even further to the west and confined to a narrower range of longitudes. The term *La Niña* (*the girl*) was coined in the mid-1980s by scientists investigating the

year-to-year oscillations between warm and cold conditions in the tropical Pacific. La Niña has also been referred to as anti-El Niño, ENSO cold event, and El Viejo (the old man). Like El Niño, La Niña typically lasts 12–18 months.

La Niña's effects on global weather variability are roughly (though not exactly) opposite to those of El Niño (Halpert and Ropelewski, 1992). The atmospheric response to weak-to-moderate cold and warm tropical Pacific sea surface temperature anomalies tends to be similar in magnitude, but opposite in sign. However, the atmospheric response to strong La Niña events tends to be weaker than the response to strong El Niño events. This difference arises because tropical rainfall (which translates into atmospheric heating and associated teleconnection patterns) has a lower limit of zero, regardless of how cold the tropical Pacific may get. On the other hand, the upper limit for rainfall and hence atmospheric heating during strong El Niño events is not as rigidly constrained.

Examples of La Niña weather impacts include an increased probability of unusually rainy conditions in southern Africa and northeastern Brazil, and in the monsoon regions of India, Indonesia and Northern Australia. La Niña is often linked to drier than normal conditions over equatorial East Africa, southern Brazil and Uruguay. The subtropical jet streams over the Pacific weaken, shift poleward, and become more variable in strength during La Niña winters. Blocking highs tend to develop in the eastern North Pacific, accompanied by more frequent cold polar air outbreaks over western North America. These changes in atmospheric pressure patterns and circulation result in winters that tend to be colder and stormier than normal over Alaska, western and central Canada, and the northern US. Conversely, the northward shift in the subtropical jet stream leads to warmer and drier than normal conditions in the southeastern US, and drier than normal conditions in the southern plains of the US.

La Niña, like El Niño, affects tropical storm frequency, intensity, and geographical distribution through changes in sea surface temperature and atmospheric circulation. Pacific hurricanes, typhoons and cyclones are more restricted in their geographical extent because of colder underlying sea surface temperatures. On the other hand, Atlantic hurricanes tend to increase in number as the subtropical jet stream shifts northward, reducing the shear between upper and lower level tropospheric winds where hurricanes form. The 1995 Atlantic hurricane season is a good example of what can happen during La Niña. That year witnessed a bumper crop of 19 named tropical Atlantic storms, including 11 hurricanes, almost double the usual number.

La Niña's socio-economic impacts can be as impressive as those resulting from El Niño. La Niña-related drought and heat waves in the US Midwest during the summer of 1988 constituted one of the worst natural disasters in US history, causing US\$40 billion in agricultural and other losses, and claiming approximately 7500 lives from heat stress. Also, with more and stronger Atlantic hurricanes during La Niña, their destructive potential and probability of making landfall in populated regions increases. For the US, it is three times more likely that an intense hurricane will make landfall during a La Niña than during an El Niño. Hurricane Mitch, one of the strongest Atlantic hurricanes on record and the deadliest in 200 years, was spawned during the 1998 La Niña. Mitch devastated Central America, claiming 10 000 lives, leaving over three million homeless, and causing US\$6 billion in damage.

La Niña can also be beneficial to some regions of the globe. For instance, higher monsoon rainfall totals over the Indian subcontinent, the western Pacific, and northeastern Brazil can support greater agricultural production and economic growth. Enhanced winter snowpack in the mountains of the Pacific Northwest provide for extra hydroelectric power production, ample summer water supplies, and improved freshwater habitat for salmon. In terms of marine ecosystems, primary productivity, driven by more intense equatorial and coastal upwelling, is generally enhanced. Higher-level marine organisms tend to thrive under these conditions, and severe disruptions in fisheries, like those during El Niño, are not so evident.

DECADAL VARIATIONS AND GLOBAL WARMING

The frequency and amplitude of El Niño and La Niña events are modulated on decadal and longer time scales. The 1930s to the early 1950s, for example, was a period of relatively few El Niños, while the period since 1976 has witnessed more frequent, stronger, and in the case of 1991–1995, longer lasting El Niños. In addition, the magnitude of the strongest El Niños over the past 50 years seems to be increasing while at the same time there has been a trend toward fewer La Niña events (Figure 3).

Variations in the ENSO cycle may simply be a result of random or chaotic fluctuations in the Earth's highly complex climate system. However, there may be other factors at work as well. Temperatures have been elevated in the tropical Pacific since the mid-1970s in association with a recently discovered, naturally occurring phenomenon known as the Pacific Decadal Oscillation, or (PDO) (Mantua *et al.*, 1997) (see **Pacific–Decadal Oscillation**, Volume 1). This oscillation alternates between phases of warm and cold tropical Pacific sea temperatures lasting 20–25 years. The physical mechanisms that account

for the PDO are at present poorly understood. However, the PDO affects the background oceanographic and atmospheric conditions on which ENSO events develop. Warm phase PDO and El Niño sea surface temperature anomalies are roughly additive. Under these conditions, the global atmospheric teleconnection patterns set up by elevated tropical Pacific sea surface temperatures can be amplified.

In addition to naturally occurring phenomena such as the PDO, global warming may also affect the ENSO cycle (Trenberth and Hoar, 1996). The warmest years on record were 1998 and 1997, in that order. Occurrence of 1997–1998 El Niño contributed in part to these extremes, because global temperatures rise a few tenths of a degree Celsius following the peak El Niño warming in the tropical Pacific. However, aside from the record warmth in 1997–1998, there has been an underlying trend toward increased globally averaged air temperatures of about 0.6 °C over the past century. Moreover, tree ring and ice core data indicate that the 20th century has been the warmest century and the 1990s has been the warmest decade over the past millennium. The consensus of the scientific community at present is that the recent increase in global temperatures is human-induced through fossil fuel combustion and deforestation (Houghton *et al.*, 1996).

It is reasonable to assume that anthropogenic greenhouse gas warming will affect ENSO because both phenomena are involved in regulating the Earth's heat balance. In addition, an altered ENSO cycle may leave its imprint on the global carbon balance (see Box 3) and on patterns of regional climate change. If global warming were to lead to intensified, more frequent, or prolonged El Niños, those regions affected by El Niño-related drought or flood in the present climate might well be more prone to such natural disasters in the future. How global warming may affect ENSO and other natural modes of climate variability is not known at present though. Computer models used for developing scenarios of how the Earth's climate will change in response to elevated levels of carbon dioxide (CO₂) and other greenhouse gases in the atmosphere differ on how the tropical Pacific Ocean will be affected (Meehl *et al.*, 2000). Many coupled ocean-atmosphere models predict a permanent El Niño-like warming of the tropical Pacific due to increased forcing from greenhouse gases. Some models also exhibit more energetic and higher frequency year-to-year ENSO-like fluctuations superimposed on this permanent warming. However, realistic greenhouse gas forcing in other models can lead to quite different scenarios. The differences among model simulations arise in part because results are very sensitive to the representation of poorly understood but critical processes such as the formation of clouds and their radiative feedbacks on the global energy balance, and the transport of heat

Box 3 El Niño and the Global Carbon Cycle (see **Carbon Cycle**, Volume 2)

Each year, seven billion tons of carbon in the form of CO₂ are released into the atmosphere from anthropogenic sources. About half this amount remains in the atmosphere, while the other half is taken up approximately equally by the ocean and the terrestrial biosphere. Ocean uptake occurs at high latitudes where the deep waters of the world's oceans form. Uptake also occurs in the subtropics where surface waters are carried down into the thermocline.

The tropical oceans are a major source of CO₂ to the atmosphere, with the Pacific Ocean dominant because of its great size. Equatorial upwelling outgases about one billion tons of carbon in the form of CO₂ per year into the atmosphere, as water rich in inorganic carbon is brought up from the thermocline to the surface. The amount of carbon released to the atmosphere in the equatorial Pacific would be even higher were it not for photosynthesis, which converts one billion tons of upwelled inorganic carbon each year into living organisms.

Year-to-year variability in global atmospheric carbon concentrations is dominated by the ENSO cycle (Rayner *et al.*, 1999). During El Niño, equatorial upwelling is suppressed in the eastern and central Pacific,

significantly reducing the supply of CO₂ to the atmosphere oceanic (Feely *et al.*, 2000). As a result, the global rise in CO₂ noticeably slows down during the early stages of an El Niño event. However, during the later stages of El Niño, global CO₂ concentrations rise sharply, possibly reflecting the delayed response of the terrestrial biosphere to El Niño-induced changes in weather patterns. Widespread droughts and elevated temperatures in the tropics during El Niño contribute to an increase in the number of forest fires, modifying the balance between respiration and photosynthetic uptake of CO₂ in land plants. These processes could result in an anomalous increase in the supply of CO₂ to the atmosphere sufficient to override the reduction in CO₂ from decreased equatorial upwelling.

In addition to year-to-year variations, lower frequency changes in the ENSO cycle can affect the global atmospheric carbon balance. In particular, the 1990s was an unusual decade in that it witnessed both a prolonged El Niño in 1991–1995 and an extraordinarily strong El Niño in 1997–1998. These El Niño events resulted in an overall decrease of oceanic input to the atmosphere of about two to three billion tons of carbon during the 1990s relative to the 1980s (Feely *et al.*, 2000).

by ocean currents and turbulent mixing. Thus, uncertainties in the simulated effects of global warming on ENSO and ENSO-like variability are large, and further model improvements are required to gain confidence in the details of future climate projections based on such simulations.

Instrumental records have also been studied extensively for clues about the relation between ENSO and global warming. Unfortunately, these records are limited to the past 100–150 years, and are too short to describe the full range of natural climatic variability on inter-annual and decadal time scales. Thus, from instrumental data alone it is not possible to unambiguously answer the question of whether the unusual character of ENSO during the past 25 years is within the range expected for natural variations, or whether it is anthropogenically forced. On the other hand, paleoclimatic reconstruction based on proxy data allow for investigation of ENSO variability from periods predating the instrumental record. For example, year-to-year fluctuations in the Earth's climate are evident in New England lake sediments dating from near the end of the last ice age (15 000 years before present) when the Earth was cooler (Rittenour *et al.*, 2000), and in fossil Pacific coral records from the last interglacial period (124 000 years before present) when the Earth was slightly warmer (Hughen *et al.*, 1999). These and other proxy records exhibit decadal modulations in the amplitude of ENSO time scale variations similar to those observed today. Moreover, compared to some coral climate reconstructions, the increased frequency and strength of El Niño

events since 1975 could be considered unusual relative to earlier epochs.

However, using paleoclimatic data as a benchmark for evaluating global warming effects in the modern ENSO record is complicated by the fact that background climatic conditions on which ENSO developed during earlier periods of the earth's history have frequently been very different from those which exist today (Tudhope *et al.*, 2001). A further complication is that there are relatively few reliable proxy records capable of defining year-to-year variations in the distant past, and those records are sparsely distributed in both space and time. Finally, the information in proxy records is subject to contamination by non-climatic chemical, biological and physical changes related to micro-environmental factors. Therefore, conclusions based on comparisons with proxy data about the effects of global warming on the ENSO cycle are subject to considerable uncertainty at this time.

CONCLUSION

The dramatic 1997–1998 El Niño highlighted progress made in ENSO research and forecasting since the pioneering work of Bjerknes nearly four decades ago. New observational techniques now allow us to take the pulse of the tropical Pacific day-by-day, and computer forecast models can predict the broad outlines of ENSO-related climatic perturbations up to one year in advance. The accuracy of these models is sufficient in some cases to

allow for practical applications of forecast information for planning and mitigation purposes.

These scientific advances, though impressive, are just the beginning. Theories and observations have illuminated many basic features of the ENSO cycle, but fundamental questions such as why the trade winds initially weaken at the onset of El Niño still appear to have no simple answer. How ENSO interacts with the PDO and how it may be affected by global warming are not at present well understood. Though satellites can monitor the globe from space, comprehensive ocean-based observational networks as required for climate research and prediction are limited primarily to the tropical Pacific. This limitation hinders attempts to examine interactions between the ocean and the atmosphere in regions outside the tropical Pacific where important physical processes may affect, or be affected by, ENSO variations.

ENSO forecast systems are in their infancy, in some ways analogous to the early stages of numerical weather forecasting 40 years ago. As might be expected, despite the many seasonal forecasting successes during 1997–1998, there were notable failures. None of the forecast models predicted the ultimate intensity of the El Niño before its onset, and one previously successful model failed completely. Similarly, predictions of severe drought in Australia and Zimbabwe, and reduced summer monsoon rainfall over India, proved to be erroneous. The reasons for these failures have yet to be fully determined.

The oscillation between warm, neutral, and cold states in the tropical Pacific associated with the ENSO cycle involves massive redistributions of upper ocean heat content. For instance, the accumulation of excess heat in the eastern Pacific due to the eastward movement of warm water and to the depression of the thermocline during a strong El Niño is approximately equivalent to the output of a million 1000 megawatt power plants operating continuously for a year. The magnitude of these natural variations clearly indicates that society cannot hope to consciously control or modify the ENSO cycle. Rather, we must learn to better predict it, and to adapt to its consequences.

The challenge for physical scientists then is to improve ENSO forecast models, to improve our understanding of underlying physical processes at work in the climate system, and to improve the observational data base in support of these objectives. Capitalizing on advances in the physical sciences for practical purposes is a challenge for social scientists, economists, politicians, business leaders, and the citizenry of those countries affected by ENSO variations. The promise of the future is that continued research on ENSO and related problems will be rewarded with scientific breakthroughs that translate into a broad range of applications for the benefit of society.

REFERENCES

- Barber, R T and Chavez, F P (1983) Biological Consequences of El Niño, *Science*, **222**, 1203–1210.
- Barnston, A G, Glantz, M H, and He, Y (1999) Predictive Skill of Statistical and Dynamical Models in SST Forecasts During the 1997–1998 El Niño Episode and the 1998 La Niña Event, *Bull. Am. Meteorol. Soc.*, **80**, 217–243.
- Canby, T Y (1984) El Niño's Ill Wind, *Natl. Geogr.*, **165**(2), 144–183.
- Changnon, S A (1999) Impacts of the 1997–1998 El Niño-Generated Weather in the US, *Bull. Am. Meteorol. Soc.*, **80**, 1819–1827.
- Feely, R A, Boutin, J, Cosca, C E, Dandonneau, Y, Etcheto, J, Inoue, H Y, Ishii, M, LeQuere, C, Mackey, D, McPhaden, M J, Metzl, N, Poisson, A, and Wanninkhof, R (2000) Seasonal and Inter-Annual Variability in CO₂ in the Equatorial Pacific, *Deep-Sea Res.*, in press.
- Glantz, M H (2001) *Currents of Change: El Niño's Impact on Climate and Society*, Cambridge University Press, Cambridge, 1–252.
- Gray, W M (1984) Atlantic Hurricane Frequency: El Niño and 30 mb Quasi-biennial Oscillation Influences, *Mon. Weather Rev.*, **112**, 1649–1668.
- Halpert, M S and Ropelewski, C F (1992) Surface Temperature Patterns Associated with the Southern Oscillation, *J. Clim.*, **5**, 577–593.
- Horel, J D and Wallace, J M (1981) Planetary Scale Atmospheric Phenomena Associated with the Southern Oscillation, *Mon. Weather Rev.*, **109**, 813–829.
- Houghton, J T, Meira Fihlo, L G, Callender, B A, Harris, N, Kattenberg, A, and Maskell, K, eds (1996) *Clim. Change (1995) The Science of Climate Change*, Cambridge University Press, Cambridge, 549.
- Hughen, K A, Schrag, D P, and Jacobsen, S B (1999) El Niño During the Last Interglacial Period Recorded by a Fossil Coral from Indonesia, *Geophys. Res. Lett.*, **26**, 3129–3132.
- McPhaden, M J (1999) Genesis and Evolution of the 1997–1998 El Niño, *Science*, **283**, 950–954.
- McPhaden, M J, Busalacchi, A J, Cheney, R, Donguy, J R, Gage, K S, Halpern, D, Ji, M, Julian, P, Meyers, G, Mitchum, G T, Niiler, P P, Picaut, J, Reynolds, R W, Smith, N, and Takeuchi, K (1998) The Tropical Ocean-Global Atmosphere (TOGA) Observing System: a Decade of Progress, *J. Geophys. Res.*, **103**, 14 169–14 240.
- Mantua, N J, Hare, S R, Zhang, Y, Wallace, J M, and Francis, R C (1997) A Pacific Inter-decadal Climate Oscillation with Impacts on Salmon Production, *Bull. Am. Meteorol. Soc.*, **78**, 1069–1079.
- Meehl, G A, Zwiers, F, Evans, J, Knutson, T, Mearns, L, and Whetton, P (2000) Trends in Extreme Weather and Climate Events: Issues Related to Modelling Extremes in Projections of Future Climate Change, *Bull. Am. Meteorol. Soc.*, **81**, 427–442.
- National Research Council (1996) *Learning to Predict Climate Variations Associated with El Niño and the Southern Oscillation. Accomplishments and Legacies of the TOGA Program*, National Academy Press, Washington, DC, 171.
- Philander, S G H (1990) *El Niño, La Niña, and the Southern Oscillation*, Academic Press, San Diego, CA, 293.

- Quinn, W H (1992) A Study of Southern Oscillation-related Climatic Activity for AD 622–1900 Incorporating Nile River Flood Data, in *El Niño – Historical and Paleoclimatic Aspects of the Southern Oscillation*, eds H Diaz and V Markgraf, Cambridge University Press, Cambridge, 119–149.
- Quinn, W H, Neal, V T, and Antunez de Mayolo, S E (1987) El Niño Occurrences over the Past Four and a Half Centuries, *J. Geophys. Res.*, **92**, 14 449–14 461.
- Ramp, S R, McClean, J L, Collins, C A, Semtner, A J, and Hayes, K A S (1997) Observations and Modeling of the 1991–1992 El Niño Signal off Central California, *J. Geophys. Res.*, **102**, 5553–5582.
- Rayner, P J, Enting, I G, Francey, R J, and Langenfelds, R (1999) Reconstructing the Recent Carbon Cycle from Atmospheric CO₂, $\Delta^{13}\text{C}$ and O₂/N₂ observations, Tellus Publications, Boston, MA, **51B**, 213–232.
- Rittenour, T M, Brigham-Grette, J, and Mann, M E (2000) El Niño-like Climate Teleconnections in New England During the Late Pleistocene, *Science*, **288**, 1039–1042.
- Ropelewski, C F and Halpert, M (1987) Global and Regional Scale Precipitation Patterns Associated with the El Niño/Southern Oscillation, *Mon. Weather Rev.*, **115**, 1606–1626.
- Sponberg, K (1999) *Compendium of Climatological Impacts*, National Oceanic and Atmospheric Administration, Washington, DC, 62.
- Strong, A E, Kearns, E J, and Govig, K K (2000) Sea Surface Temperature Signals from Satellites – an update, *Geophys. Res. Lett.*, in press.
- Supplee, C (1999) El Niño/La Niña, *Nat. Geo.*, **195**(3), 72–95.
- Trenberth, K E and Shea, D J (1987) On the Evolution of the Southern Oscillation, *Mon. Weather Rev.*, **115**, 3078–3096.
- Trenberth, K E and Hoar, T J (1996) The 1990–1995 El Niño–Southern Oscillation Event: Longest on Record, *Geophys. Res. Lett.*, **23**, 57–60.
- Trenberth, K E, Branstator, G W, Karoly, D, Kumar, A, Lau, N C, and Ropelewski, C (1988) Progress During TOGA in Understanding and Modeling Global Teleconnections Associated with Tropical Sea Surface Temperatures, *J. Geophys. Res.*, **10**, 14 291–14 324.
- Tudhope, A W, Chilcott, C P, McColloch, M T, Cook, E R, Chappell, J, Ellam, R M, Lea, D W, Lough, J M, and Shimmeld, G B (2001) Variability in the El Niño–Southern Oscillation through a glacial-interglacial cycle, *Science*, **291**, 1511–1517.
- WMO (1999) *The 1997–1998 El Niño Event: a Scientific and Technical Retrospective*, WMO No. 905, World Meteorological Organization, Geneva, Switzerland, 93.
- Wyrski, K (1975) El Niño – The dynamic response of the equatorial Pacific Ocean to Atmospheric Forcing, *J. Phys. Oceanogr.*, **5**, 572–584.